New Decline Pattern of Filtrate Flux in Cross-flow Microfiltration of Dilute Suspension

Toshiro Murase and Than Ohn
Dept. of Chemical Engineering, Nagoya University, Nagoya 464-01, Japan

The cross-flow microfiltration flux is assumed to fall smoothly with a decreasing slope from startup to the steady state. Under actual operating conditions beyond a critical level, however, an anomalous decline pattern arises; initially cross-flow medium filtration occurs and then thin-cake filtration. At the earlier stage, fine particles in polydispersed suspensoids are filtered out on the surface of the membrane and/or captured within the latter, clogging the membrane pores gradually. After the membrane surface is covered by the deposit, further filtration occurs by the buildup of filter cake on the initial deposit. Among the many operating variables, three major controlling factors for the earlier stage are confirmed: solids concentration, relative size of solids and pores, and relative force of sweeping and capturing of suspensoids. Because suspended solids are separated by medium- and cake-law filtration in a series, a method for evaluating the time dependence of flux with the new pattern is derived. Reliable flux analysis is achieved for the transient flux of the dilute suspension forming a low compressibility fouling layer, which helps understand efficient flux performance.

Introduction

The cross-flow filtration operation has been widely applied for efficient micro- and ultrafiltration. In recent years, much work on both microfiltration and ultrafiltration has been done in order to quantify the influence of the process parameters on membrane fouling and filtrate flux (Baker et al., 1985; Rautenbach, 1988; Ramero and Davis, 1988; Jordhan and Ladva, 1989; Mackley and Sherman, 1992; Bashir and Reuss, 1992; Dharmappa et al., 1992; Blake et al., 1992; Akay and Wakeman, 1993; Lu et al., 1993; Redkar and Davis, 1993; Stamatakis and Tien, 1993; Tarleton and Wakeman, 1994; Wakeman, 1994). Some researchers have addressed the filtration of particulate, mineral-based or -related suspensions; others, the filtration of biological or related suspensions. Regarding the flux performance, it is common knowledge that without membrane cleaning the decline curve falls steeply, becoming a gradually decreasing slope after operation starts until a steady state is attained (Porter, 1990).

Recently, however, it has been experimentally observed that such a conventional flux pattern is not perfectly valid for all such operations. For instance, when the pores in a ceramic membrane are much larger than the size of the suspended particulate solids (Murase et al., 1991) and the pores in a polymeric membrane are on an order of magnitude equal to baker's yeast suspensoids (Nakanishi and Tanaka, 1993), inspection of the cross-flow filtration data indicates an anomalous flux decline. Even with the ceramic membrane having a much smaller pore size than the particle size of polymethyl methacrylate (PMMA) suspensoids, under operating conditions beyond a critical level, the filtrate flux follows a new pattern: a decline curve composed of two parts with quite different slopes. That is, there appear to be two apparent filtration mechanisms governing flux decline, and the relative contributions of these mechanisms depend mostly on the process parameters. Also, this decline mode is marked by high transient flux under a constant steady flux, indicating a high probability of achieving high filtration efficiency by controlling the first stage. Furthermore, such a flux decline can also be recognized for the other system of rotational dynamic microfiltration with oil-in-water emulsion, and may be viewed as another fundamental behavior similar to the conventional one. Therefore, further analysis of such findings is strongly desirable for an understanding of the full picture of flux performance and membrane fouling in cross-flow filtration.

Correspondence concerning this article should be addressed to T. Murase.

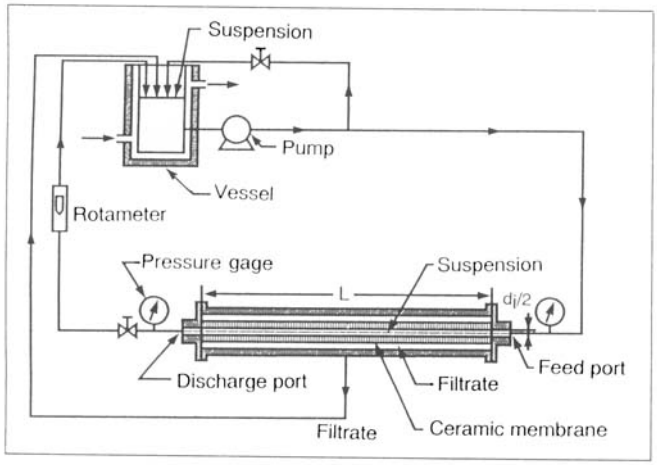

Figure 1. Experimental apparatus.

This article reports on a study of the details in the microfiltration flux with the new decline pattern, and on the effects of the operational factors on the appearance of the pattern. Also investigated is a method for evaluating the flux decline during the whole process where two different filtration mechanisms are in series.

Experimental Studies

Figure 1 shows the experimental apparatus. The filter medium used was a tubular ceramic membrane (NGK Co., Nagoya),—length $L = 50.0$ cm, outer diameter $d_o = 10.0$ mm, inside diameter $d_i = 7.0$ mm—that has a skin layer of nominal pore size $d_m = 0.2$ μm on the inside surface of the filtration area $A = 105.7$ cm^2. To be exact, the pore size ranges from 0.072 to 0.19 μm, its mean size being 0.18 μm. The material of polydispersed suspension used was PMMA particles (Soken Chemical and Engineering Co., Tokyo) with average diameter $d_p = 0.4$, 1.0, and 7.0 μm and density $\rho_s = 1{,}050$ kg/m^3, which was suspended in pure water and/or an aqueous saccharose solution at a solids mass fraction of $s = 6.23 \times 10^{-4}$–3.24×10^{-3} and a liquid viscosity of $\mu = 0.93 \times 10^{-3}$–$9.49 \times 10^{-3}$ Pa·s. In Table 1 the cumulative distribution of undersize particles is tabulated for the 0.4- and 7.0-μm materials.

After an amount of the suspension was fed into a vessel equipped with an agitator and a temperature controller, the filter system was filled with the suspension by a centrifugal pump. While the suspension was flowed axially at a constant rate through the cylindrical filter chamber, compressed gas was used to filter the suspension under constant pressure. The filtrate volume v permeated through the membrane was recorded as a function of time θ, using an electric balance and a timer. The cross-flow rate and filtration pressure were also measured by a rotameter and two pressure gages, respectively, at the feed and discharge port of the chamber. To examine the effects of operating variables on flux decline, measurements were carried out at different cross-flow rates, feed concentrations, liquid viscosities, and filtration pressures. The range of cross-flow velocity $u_c (= 4Q/\pi d_i^2)$ used in this experiment was 2.02 ~ 3.90 m/s, and the applied filtration pressure $p (= (p_A + p_B)/2)$ was 98 ~ 262 kPa. The suspension and filtrate flowing out of the cross-flow filtration cell were recycled to the vessel, and the feed concentration and temperature of the suspension were kept constant throughout each experiment.

Table 1. Cumulative Distribution of Undersize Particles

Particle Size μm	Cumulative Fraction $d_p = 0.4$	$d_p = 7.0$
20.1	1.000	0.999
10.7	1.000	0.884
7.75	1.000	0.634
5.07	1.000	0.352
2.41	1.000	0.236
1.03	0.994	0.153
0.75	0.960	0.113
0.55	0.816	0.071
0.26	0.176	0.012
0.19	0.042	0.004
0.14	0.001	0.001
0.12	0.001	0.000
0.11	0.000	

In addition, dead-end microfiltration experiments were also conducted to evaluate the filtration coefficient, K_v, of the constant pressure in batch operation.

New Decline Pattern

With the suspension of the relatively high concentration shown in Figure 2, cross-flow microfiltration proceeds on the principle of the so-called thin-cake filtration (Tiller and Cheng, 1977) across the whole process. The flux decline shows a well-known common feature, namely, the filtrate flux begins to decrease linearly just after operation starts. At the very outset, the growth rate and the hydraulic resistance of the fouling cake layer are almost the same as those for the dead-end filtration with stationary suspension. Then, the decline shows a curvilinear relation with a decreasing slope, and gradually approaches a final steady state as filtration progresses. The increasing rate of cake resistance, R_d, decreases steeply with time, as shown in Figure 3, and its value becomes much smaller than that in the dead-end filtration because of the impeded growth of the fouling cake-layer owing to the cross-flow. In view of the time dependence of the resistance, R_d, the flux decline can be expressed as

$$q = p/\mu(R_d + R_0). \tag{1}$$

Introducing a thin-cake filtration coefficient, j_d, defined as the cake-resistance ratio R_s/R_d of dead-end to cross-flow filtration, and substituting the cake resistance, $R_s = 2pv/\mu K_v$, of the dead-end filtration, one gets (Murase et al., 1991):

$$1/q = \mu R_d/p + 1/q_0 = 2v/j_d K_v + 1/q_0, \tag{2}$$

where

$$K_v = 2(1 - ms)p/\mu\alpha\rho s \tag{3}$$

$$q_0 = p/\mu R_0. \tag{4}$$

The symbol m is the ratio of wet to dry cake mass; q_0 the flux at the beginning of operation; R_0 the hydraulic resis-

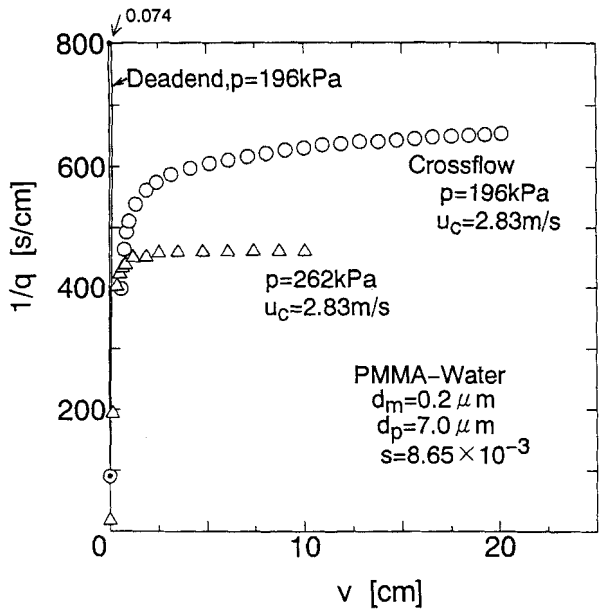

Figure 2. Conventional pattern of reciprocal flux curve.

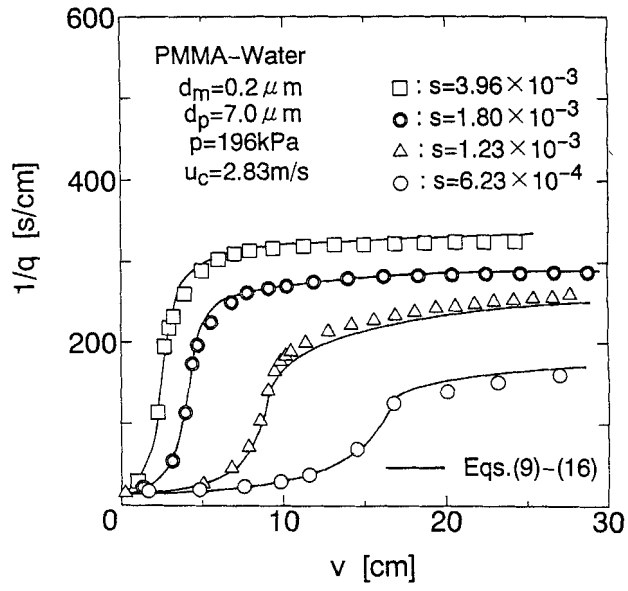

Figure 4. New pattern of reciprocal flux curve.

tance of the membrane; α the average specific resistance of cake; and ρ the density of the filtrate. In consideration of the fact that the initial slope $G_0 = [d(1/q)/dv]_{v=0}$ of the cross-flow filtration curve is nearly equal to the slope $2/K_v$ of the dead-end filtration line, the cross-flow filtration flux can be also given by

$$1/q = G_0 v/j_d + 1/q_0. \tag{5}$$

When some process parameters, such as solids mass fraction, suspended solids size, and liquid viscosity, pass some critical level, the pattern of the flux decline curve is much different from the conventional pattern, as illustrated in Figures 4 and 5. That is, the new pattern is sigmoidal in time, its curve exhibiting rising and falling slopes in the plots of reciprocal flux. Presumably, at the earlier stage of $0 < v \leqq v_1$, cross-flow medium filtration arises from the progressive pore clogging due to the sieving of suspended solids on the membrane pore and the capture of ultrafine suspensoids inside the pore structure. When the pore at the membrane surface is almost covered with the solids, thin-cake filtration successively occurs as the cake forms on the earlier deposit. Then, a steady state is attained at $v > v_2$, yielding substantial constant cake-resistance. Therefore, in view of the existence of the two filtration mechanisms in a series, the flux decline over the whole process should be represented in the form:

$$q = F(v) \qquad \text{at } v \leqq v_1 \tag{6}$$

$$q = p/\mu(R_d + R_1 + R_0) \qquad \text{at } v > v_1, \tag{7}$$

where $F(v)$ is the function of the flow rate equation for the

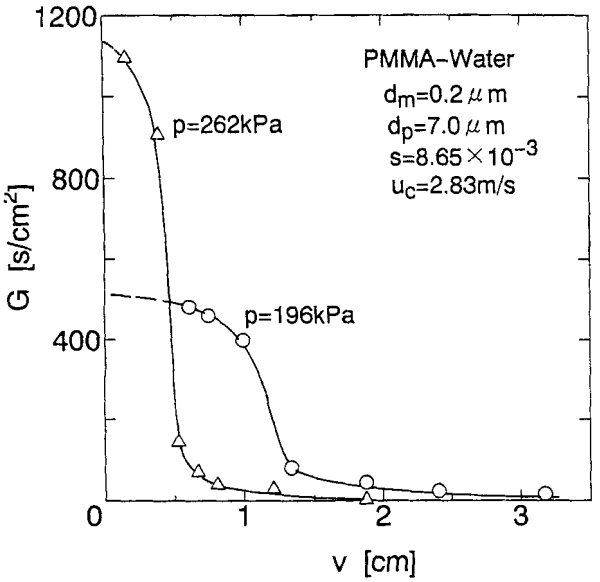

Figure 3. Time-dependent change in the gradient of reciprocal flux curve with conventional pattern.

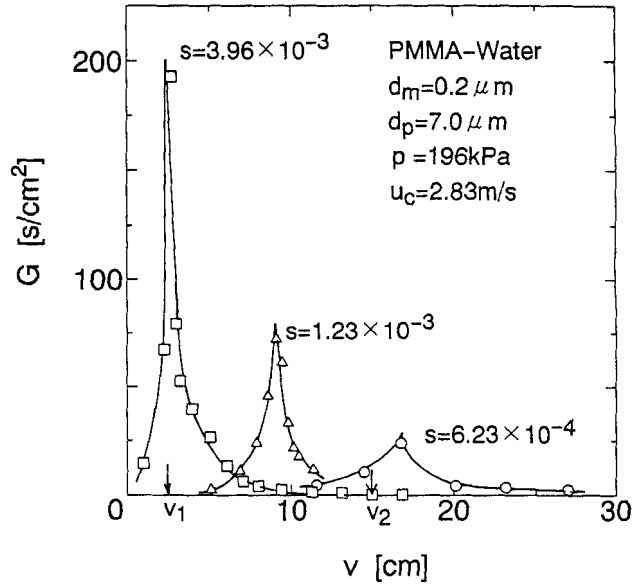

Figure 5. Time-dependent change in the gradient of reciprocal flux curve with new pattern.

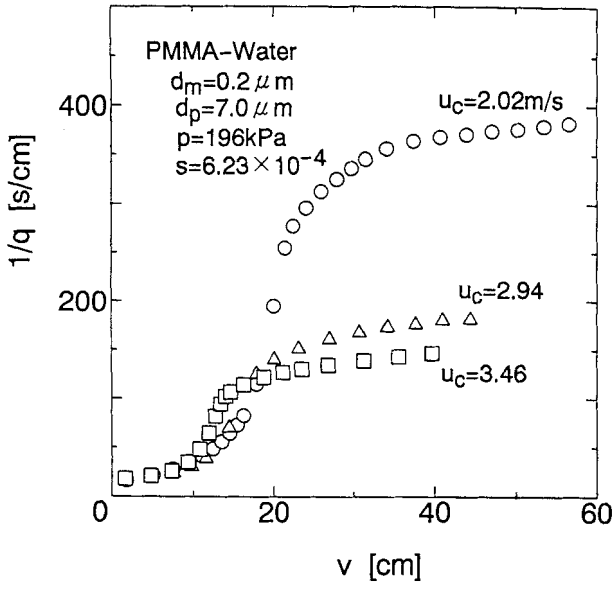

Figure 6. Effects of cross-flow velocity on medium filtration stage.

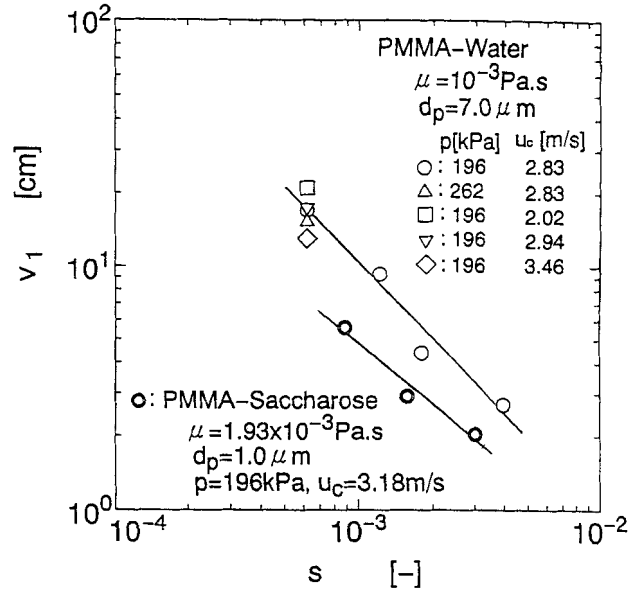

Figure 7. Dependence of critical filtrate volume v_1 on operating variables.

cross-flow medium filtration, and R_1 and v_1 denote the filtration resistance and the filtrate volume at the transition point from the first to the second stage, respectively. Since the details of such filtration behavior is quite uncertain, the controlling factors for the cross-flow medium filtration stage are shown below, and then a method for quantifying the flux decline in terms of operational parameters is presented.

Controlling Factors for Cross-flow Medium Filtration

Figures 2 to 5 show the effects of solids concentration on the flux decline. With the relatively high concentration of $s = 8.65\times10^{-3}$, the flux decreases in accordance with the conventional pattern, and its decline over the whole process is due to the thin-cake filtration mechanism, that is, the solids are swept by the cross-flow stream into the cake that has formed on the membrane, which filters them out. On the other hand, with the lower concentration below $s = 3.96\times10^{-3}$, the decline curve has a different pattern composed of the two parts of the medium and the thin-cake filtration stages. The medium filtration stage expands with the reduction of the feed concentration s.

Figure 6 shows the effects of cross-flow velocity u_c on the flux decline mode, which has a medium filtration stage. Undoubtedly, the duration of this stage varies with the velocity u_c to a much smaller extent than the final steady flux, though the stage slightly expands with a lower velocity u_c. Assuming that the transition point from the first to the second stage is equivalent to the intersection of the two parts of the curve with rising and falling slopes, as illustrated in Figure 5, the critical filtrate volume v_1 is graphically evaluated, and is plotted against the concentration s in Figure 7. Apparently, in addition to the cross-flow velocity u_c, the applied pressure p can also be regarded as minor factor. On the other hand, the concentration s can be considered to be a major factor governing the appearance of the new decline pattern. With the extrapolation of the curve to the abscissa ($v_1 = 0$) in rectangular coordinates, the critical concentration, s_c, at which the medium filtration arises, can be roughly predicted to be $(8-10)\times10^{-3}$ for the PMMA–water suspension with the suspensoids $d_p = 7.0$ μm.

Figure 8 shows the influence of the suspended material itself on the flux pattern in plots of the reciprocal flux. The solids concentration s is 6.23×10^{-4}, at which point the new decline pattern is obtained from the suspension of $d_p = 7.0$ μm. With the fine suspensoids of $d_p = 0.4$ and 1.0 μm, the flux decline follows the conventional pattern, and thus the critical concentration s_c is most likely much smaller with decreasing solids size. It is deduced that, because of the small size distribution, that allows scant possibility of filtering fine solids, the deposit at the medium filtration stage is seen in the 0.4- and 1.0-μm suspensions more frequently than in the 7.0-μm suspension. Even for such suspensions with fine solids, however, when the liquid is of high viscosity, a medium filtration stage occurs at relatively high concentrations of $s = 9.11\times10^{-4}$ and 3.20×10^{-3}, as shown in Figure 9. According to the empirical v_1 values for the suspension of $\mu = 1.93\times10^{-3}$ Pa·s, plotted in Figure 7, the high viscosity of the filtrate produces the remarkable rise in critical concentration s_c, which results in a large expansion of the medium filtration stage.

Correlation for the Prediction of Flux Decline

Cross-flow medium filtration ($0 < v \leqq v_1$)

As already noted, this stage comes from progressive pore clogging, and the flux decline may be correlated with the operational parameters on the basis of the medium blocking-law developed for dead-end processing. Therefore, assuming that at the medium filtration stage the suspended solids are captured both on the membrane surface and inside the membrane pore structure and the so-called intermediate blocking-law (Hermia, 1985) is valid, the function $F(v)$ for the transient flux at $v \leqq v_1$ is represented as:

$$q = F(v) = q_0 \exp(-k_i v), \tag{8}$$

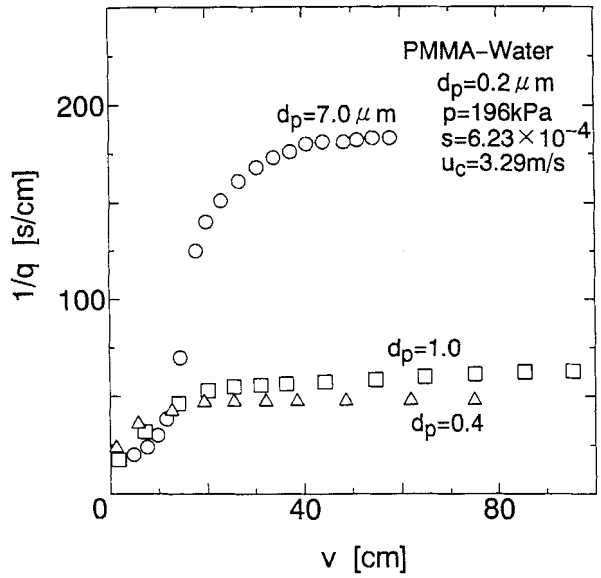

Figure 8. Effects of suspensoids size on flux decline pattern.

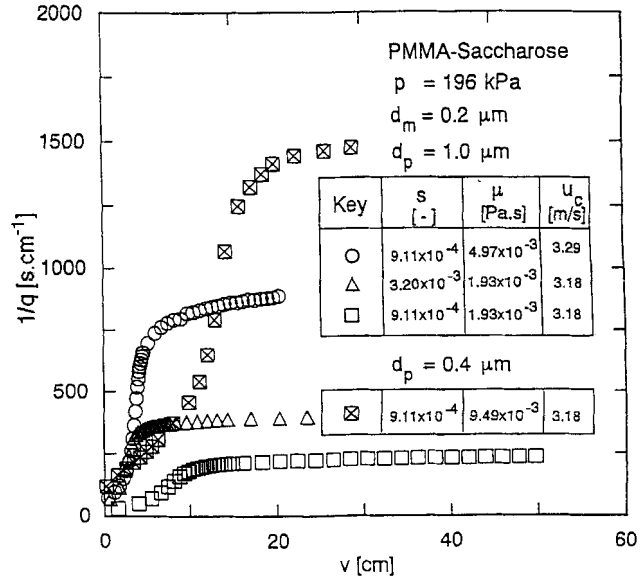

Figure 9. Effects of filtrate viscosity on medium filtration stage.

where k_i denotes the medium filtration coefficient. In the dead-end operation, the k_i value is substantially constant during a relatively short period, whereas in the cross-flow operation its value is presumably a function of elapsed time due to the cross-flow effects on the filtration. To investigate its time dependence, the coefficient k_i is evaluated from the calculation based on the substitutions of the experimental data of (q_0/q) vs. v into Eq. 8, and is plotted against the filtrate volume v in Figure 10. According to its linear relationship in the logarithmic graph, the flux decline can be rewritten as

$$1/q = \exp(k_i v)/q_0, \tag{9a}$$

where

$$k_i = \kappa_0 + \kappa_1 v^{n_k}, \tag{9b}$$

where κ_0, κ_1, and n_k are empirical constants that depend on such operating parameters as the solids concentration, the suspensoids size, and the liquid viscosity. Differentiating Eq. 9 to analyze the flux decline at a later stage, one gets

$$G_1 = q_0^{-1}[(k_i + \kappa_1 n_k v^{n_k})\exp(k_i v)]_{v=v_1}, \tag{10}$$

where G_1 is the gradient $[d(1/q)/dv]_{v=v_1}$ at the transition point of $v = v_1$.

Thin-cake filtration ($v_1 < v \leqq v_2$)

This second stage progresses with the impeded cake growth on the initial deposit, and the flux decline depends on the increase in cake resistance R_d. Assuming that substitution of the flux gradient G_1 for G_0 in Eq. 5 gives a transient cake resistance of $R_d = (G_1 pv/\mu j_d)$, the flux decline at $v_1 < v \leqq v_2$ can be represented as

$$1/q = G_1(v - v_1)/j_d + 1/q_1 \tag{11}$$

where

$$q_1 = p/\mu(R_0 + R_1) \tag{12}$$

$$R_1 = R_0[\exp(k_i v_1) - 1]_{v=v_1}. \tag{13}$$

In the preceding equation, q_1 and R_1 refer to the flux and the resistance at the filtrate volume v_1, respectively.

Figure 11 shows the empirical value of j_d, which was evaluated by substituting the measured values of G_1, q, q_1, and $(v - v_1)$ into Eq. 11. As may be seen in the figure, the coeffi-

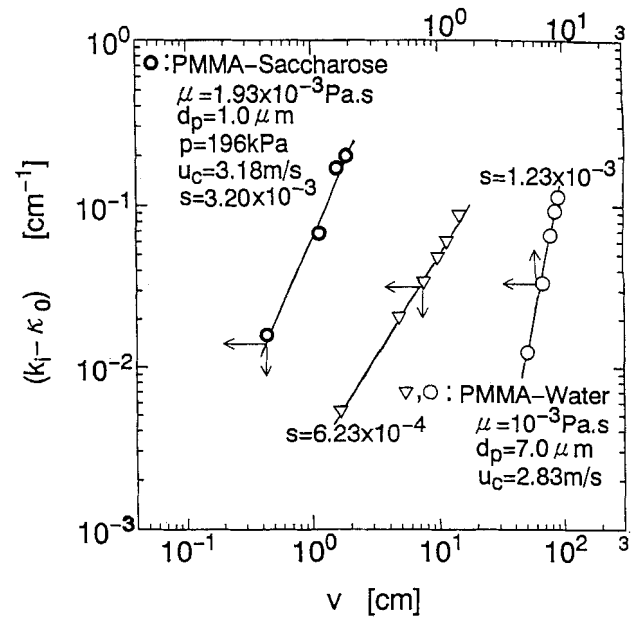

Figure 10. Time-dependent change in cross-flow medium filtration coefficient k_i.

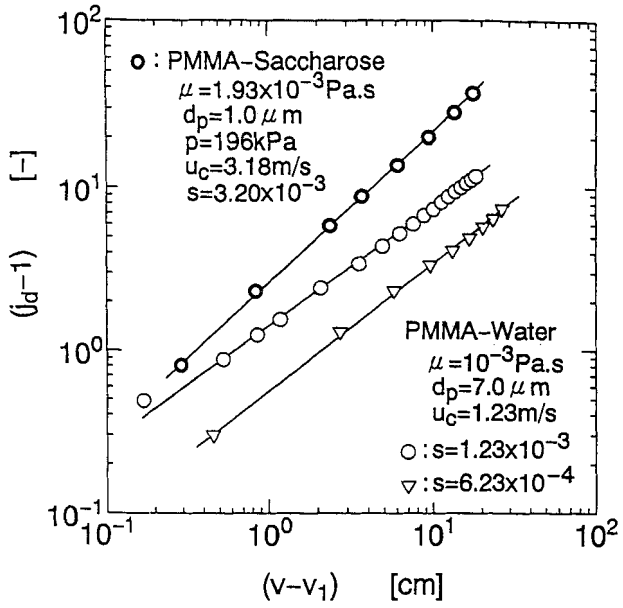

Figure 11. Time-dependent change in thin-cake filtration coefficient j_d.

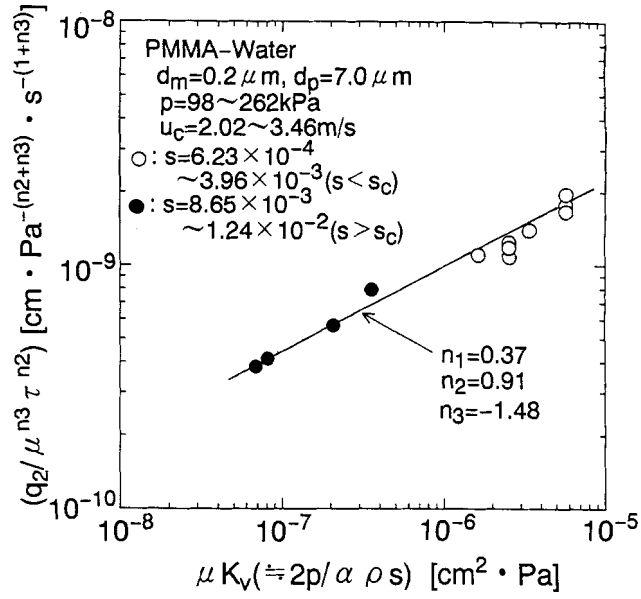

Figure 12. Correlation of steady-state flux and operating parameters.

cient j_d exceeds 1 in accordance with the following correlation:

$$j_d = 1 + k_j(v - v_1)^{n_j}, \tag{14}$$

where the empirical constant k_j is a measure of the cross-flow effects on filtration rate in the second stage. Combining Eq. 11 with Eq. 14, and assuming that $q \to q_2$ as $v \to v_2$, yields the k_j-value in the form:

$$k_j = G_1(1/q_2 - 1/q_1)^{-1}(v_2 - v_1)^{(1-n_j)}, \tag{15}$$

where v_2 denotes the filtrate volume at the point where the steady-state flux q_2 is attained. Considering that the changing rate G of the reciprocal flux becomes less than about 1 s/cm^2 at the steady state, the v_2 value can be easily evaluated as shown in Figure 5.

Steady state ($v > v_2$)

In the traditional cross-flow microfiltration without the medium filtration stage, steady flux q_2 shows a linear relation in each of the logarithmic plots against both the liquid viscosity μ and the shear stress τ acting on the cake surface (Murase et al., 1995). On the basis of these graphical confirmations, all the experimental data of the 7.0-μm suspension are plotted as $(q_2/\mu^{n_3}\tau^{n_2})$ vs. $(\mu K_v)^{n_1}$ in Figure 12, where the liquid viscosity μ ranges from 9.3×10^{-4} to 1.1×10^{-3} Pa·s. The hollow and black dots denote the data in the flux pattern with and without medium filtration stage, respectively. In preparing the graph, the coefficient K_v and the stress τ were evaluated, respectively, from the calculations based on the linearity of $1/q$ vs. v in the dead-end filtration, and based on measurements of the pressure drop $(p_A - p_B)$ through the filter chamber. Whether the cross-flow medium filtration occurs or not, with the three main parameters K_v, τ, and μ, the steady-state flux q_2 can be related to a number of operating variables as

$$q_2 = CK_v^{n_1}\tau^{n_2}\mu^{n_4}, \tag{16}$$

where $n_4 = n_1 + n_3$, and C is an empirical constant. The exponents n_1 to n_4 are the filtration characteristics of the material itself. The empirical equation, Eq. 16, is similar to that of the other systems with a conventional flux pattern, such as the cross-flow microfiltration of the suspension that forms a highly compressible fouling layer (Murase et al., 1995) and the rotating dynamic microfiltration of both the high viscosity suspension (Murase et al., 1992) and the O/W emulsion. According to the preceding analysis, the steady and transient flux over the whole process can be estimated on the basis of Eqs. 9 to 16, even though the cross-flow microfiltration process has two stages due to the different filtration mechanisms. The calculated values compared favorably with the experimental data in Figure 4.

Conclusion

To illuminate the new flux decline, which has been quite overlooked, the operational factors governing its decline pattern were examined. A method for correlating the flux decline with operational variables was proposed.

In the polydispersed suspension with the lower concentration below a critical level, reciprocal flux is sigmoidal in time as opposed to that observed conventionally, its behavior indicating that there are two stages: cross-flow medium filtration and thin-cake filtration. The former is due to progressive clogging of membrane pores, and its appearance is strongly dependent on the operating variables of suspensoids size, pore size, and liquid viscosity, as well as the concentration of the solids. On the other hand, the latter occurs when the thin-cake forms on the initial deposit, and the flux decline is related to different process conditions expressed in terms of

constant pressure filtration coefficient, shear stress at the cake surface, and liquid viscosity. According to these correlations, the flux over the whole process can be well evaluated on the basis of both medium-law and cake-law filtration equations, in a way similar to the evaluation for the conventional pattern without the medium filtration stage. Reliable flux analysis can be achieved even for the suspension by using two different mechanisms in a series. Considering that the new flux decline is distinguished in high transient flux from the conventional one, the analysis can be efficient as a basis both for the design of high rate filtration and for understanding the details of cross-flow filtration behavior.

Acknowledgment

This work was performed under a Grant-in-Aid for scientific research, no. 07650891, Japan.

Notation

k_j = empirical constant in Eq. 14, m^{-n_j}
p_A = hydraulic pressure at feed port, Pa
p_B = hydraulic pressure at discharge port, Pa
Q = volumetric cross-flow rate of suspension, $m^3 \cdot s^{-1}$
q = filtrate flux at a time θ, $m \cdot s^{-1}$

Literature Cited

Akay, G., and R. J. Wakeman, "Ultrafiltration and Microfiltration of Surfactant Dispersions—An Evaluation of Published Research," *Trans. Ind. Chem. Eng.*, **71**(A), 411 (1993).

Baker, R. J., A. G. Fane, C. J. D. Fell, and B. H. Yoo, "Factors Affecting Flux in Crossflow Filtration," *Desalination*, **53**, 81 (1985).

Bashir, I., and M. Reuss, "Dynamic Model for Crossflow Microfiltration of Microbial Suspension in Porous Tubes," *Chem. Eng. Sci.*, **47**, 189 (1992).

Blake, N. J., I. W. Cumming, and M. Streat, "Prediction of Steady State Crossflow Filtration Using a Force Balance Model," *J. Memb. Sci.*, **68**, 205 (1992).

Dharmappa, H. B., J. Verink, R. Ben Aim, K. Yamamoto, and S. Vigneswaran, "A Comprehensive Model for Crossflow Filtration Incorporating Polydispersity of the Influent," *J. Memb. Sci.*, **65**, 173 (1992).

Hermia, J., *Blocking Filtration*, A. Rushton, ed. Nijhoff, Lancaster, Pa. (1985).

Jordham, E. J., and H. K. J. Ladva, "Crossflow Filtration of Bentonite Suspension," *Phys. Chem.* **Hydrodyn.**, **11**, 411 (1989).

Lu, W. M., K. J. Hwang, and S. C. Ju, "Study on the Mechanism of Crossflow Filtration," *Chem. Eng. Sci.*, **48**, 863 (1993).

Mackley, M. R., and N. E. Sherman, "Crossflow Cake Filtration," *Chem. Eng. Sci.*, **47**, 3067 (1992).

Murase, T., C. Pradistsuwana, E. Iritani, and K. Katsumi, "Dynamic Microfiltration of Dilute Slurries with a Rotating Ceramic Membrane," *J. Memb. Sci.*, **62**, 187 (1991).

Murase, T., D. W. Yang, and E. Iritani, "Microfiltration Characteristics of High-Viscosity Slurries in Rotating Dynamic Filter," Kagaku Kogaku Ronbunshu, **18**, 708 (1992).

Murase, T., T. Ohn, and K. Kimata, "Filtrate Flux in Microfiltration of Dilute Suspension Forming a Highly Compressible Fouling Cake-Layer," *J. Memb. Sci.*, **108**, 121 (1995).

Nakanishi, K., and T. Tanaka, "Crossflow Filtration of a Microbiological Culture Suspension," *Chem. Eng.*, **38**, 21 (1993).

Porter, M. C., *Handbook of Industrial Membrane Technology—Microfiltration*, Noyes Press, Park Ridge, NJ, p. 61 (1990).

Ramero, C., and R. H. Davis, "Global Model of Crossflow Microfiltration in Membrane Operation Process," *J. Memb. Sci.*, **39**, 157 (1988).

Rautenbach, R., "Ultrafiltration of Macromolecular Solution and Crossflow Microfiltration of Colloidal Suspension," *J. Memb. Sci.*, **36**, 231 (1988).

Redkar, S. G., and R. H. Davis, "Crossflow Microfiltration of Yeast Suspensions in Tube Filters," *Biotechnol. Prog.*, **9**, 625 (1993).

Stamatakis, K., and C. Tien, "A Simple Model of Crossflow Filtration Based on Particle Adhesion," *AIChE J.*, **39**, 1292 (1993).

Tarleton, E. S., and R. J. Wakeman, "Understanding Flux Decline in Crossflow Microfiltration: Effects of Process Parameters," *Trans. Ind. Chem. Eng.*, **71**(A), 431 (1994).

Tiller, F. M., and K. S. Cheng, "Delayed Cake Filtration," *Filtr. Sep.*, **14**, 13 (1977).

Wakeman, R. J., "Visualization of Cake Formation Crossflow Microfiltration," *Trans. Ind. Chem. Eng.*, **72**(A), 530 (1994).

Manuscript received July 31, 1995, and revision received Nov. 6, 1995.